

Giuseppe Maurizio Gagliardi<sup>1</sup>, Mandar D. Kulkarni<sup>2</sup> & Francesco Marulo<sup>1</sup>

<sup>1</sup>Department of Industrial Engineering, University of Naples Federico II, Naples, Italy <sup>2</sup>Department of Aerospace Engineering, Embry-Riddle Aeronautical University, Daytona Beach, Florida, US

#### **Abstract**

Accurate and efficient sensitivity analysis is fundamental for the convergence of gradient-based optimization techniques. Analytical sensitivity methods are preferred over numerical ones for their accuracy and higher computational efficiency. Although analytical sensitivity methods have been developed for different static structural and purely aerodynamic problems, no methods exist for flutter shape eigensensitivities. This work presents the development of semi-analytical methods for calculating the sensitivity of flutter eigenvalues to variations in the structural and aerodynamic shape simultaneously. A discrete analytical differentiation of the flutter governing equations has been performed. Existing discrete analytical methods are developed for eigenvalue problems formulated in the node set. A novel methodology is introduced to handle flutter equations written in modal coordinates. The technique requires the differentiation of the structural and aerodynamic matrices and the real eigenvectors matrix. The derivative of the structural mass, stiffness, and damping matrices has been calculated analytically with an element-agnostic approach. On the other hand, aerodynamic matrices have been differentiated using finite differences, leading to a semi-analytical sensitivity method. The proposed methodology yields promising results, demonstrating the analytical differentiability of flutter eigenvalues and paving the way to a more accurate aeroelastic tailored design.

**Keywords:** Analytical sensitivity methods, Discrete analytical differentiation, Shape optimization, Flutter eigensensitivities, Aeroelasticity

#### 1. Introduction

In the realm of modern aircraft design, addressing a proper structural and aerodynamic shape is crucial for ensuring strength, control, and performance aspects. To fully comprehend the implications of these factors, reliable and accurate aeroelastic sensitivity analysis is necessary. Among the various aeroelastic characteristics, flutter sensitivities pose greater complexity and difficulty [1]. Moreover, the shape sensitivities of flutter characteristics present even greater challenges. This is primarily due to the nonlinear relationship between the mass and stiffness matrices of the aeroelastic system and the shape design variables, in contrast to the linear relationship with sizing-type design variables [2]. Consequently, the finite difference method is inadequate for accurately solving shape sensitivities.

# 1.1 Aeroelastic shape optimization

Few works exist on analytical methods for aeroelastic shape sensitivity. The bibliography on the topic can be subdivided into two main categories:

Fully analytical sensitivity methods for simplified models, such as analytical beams or springs
as structural components, and bidimensional sections as aerodynamics. While they are scientifically significant and demonstrate the possibility of analytically differentiating aeroelastic
problems, they do not find practical applications for real aeroelastic shape optimization problems.

• Detailed three-dimensional (3D) finite element models with quasi-steady aerodynamics based on Computational Fluid Dynamics (CFD) calculations solving Euler equations at each stage. Even if the structure is more accurate and detailed, this kind of model does not find practical applications in aircraft design since the structure is not yet designed and only an overall estimation of the stiffness is available. Often, finding the overall structural characteristics is the scope of the optimization itself. The same goes for aerodynamics which is based on CFD simulations of 3D geometries. The detailed aerodynamic geometry of an aircraft prototype is not available in the design phase as the scope of the aeroelastic shape optimization tools is finding the main geometric characteristics of the surfaces (length, chord, aspect ratio, sweep angle). Finally, optimizing this kind of model is computationally challenging, especially considering that multiple optimizations are necessary during the aircraft design phase.

Additionally, both methodologies are developed in the time domain while common aeroelastic solutions are in the frequency domain. The present work perfectly fits in this framework providing a shape sensitivity method in the frequency domain and consistent with the aeroelastic models actually used for aeroelastic shape optimizations. Flutter eigenvalue sensitivity allows to find significant information for the optimization, such as damping or flutter speed sensitivities. Instead, sensitivities in the time domain are not practically significant. During the design phase of a new aircraft, stick-beam structural models and Doublet Lattice Method (DLM) aerodynamics are commonly employed models [3]. However, no analytical sensitivity methods are available for this kind of model. Furthermore, one of the widely used software for flutter analysis and optimization (MSC/Simcenter NASTRAN) only permits structural parameters to be considered as design variables [4], not allowing a proper aeroelastic optimization. If the sensitivity for structural parameters is limited, the optimization of shape design parameters is not possible at all. Consequently, this work addresses this gap by introducing an accurate and efficient sensitivity method for aeroelastic sensitivity analysis. Additionally, it enables the optimization of both structural and aerodynamic shape parameters, thereby facilitating proper aeroelastic shape optimization.

In the following, a comprehensive overview of the existing research conducted in the field of analytical aeroelastic shape optimization is provided.

Kulkarni et al. [5] employed the multiphysics capabilities of Stanford University Unstructured (SU2) [6] software to obtain an analytical aeroelastic sensitivity. A bidimensional NACA 0012 airfoil has been employed for the aerodynamic part, whose shape has been considered as a design variable. The airfoil has been connected to a string (beam) to simulate the structural part. Quasi-steady CFD aerodynamics has been employed. Two previous works [7, 8] obtained similar results with a simplified section aerodynamics theory. These works aimed to apply Continuum Sensitivity Analysis (CSA) to (nonlinear) gust response problems. Canfield and Sandler [9] recently applied the CSA method to the transient gust response of a two-dimensional airfoil in a compressible flow, flexibly attached to a rigid body mass. They developed for the first time the method in an arbitrary Lagrangian-Eulerian reference frame. The aerodynamics has been modelled using Euler equations.

Maute et al. [10] considered the problem of optimizing steady-state conditions of an aeroelastic system, by varying both aerodynamic and structural parameters such as the shape of the dry or wet surface, and the orientation of the composite fibres. A detailed 3D finite element model for the structure and a 3D Euler finite volume method for the fluid were employed. Subsequently, fast parallel staggered algorithms for evaluating the aeroelastic responses and computing the analytically derived gradients of the optimization criteria were employed [11]. A subsequent work [12] also considers nonlinearity in the aeroelastic solution, employing nonlinear Euler equations for aerodynamics. Blair et al. [13] optimized and designed a joined-wing aircraft configuration. They employed CFD simulations for aerodynamics and optimized stiffness and mass structural parameters instead of shape ones. In the Yang study [1], the equivalent plate model and piston theory are used to construct the aeroelastic model, and Lancaster's adjoint method is used to compute eigenvalue sensitivities and flutter shape sensitivities. However, this method employs a simplified aerodynamics of a plate geometry in the supersonic field ( $M \gg 1$ ). Again, this method is not suitable for DLM aerodynamic theory.

A couple of works employ an aerodynamic theory more similar to the one effectively used in common aeroelastic optimization models, but still in the time domain. Stewart et al. optimized the shape

of a plate-like flapping wing [14]. The aeroelastic system is made by coupling an unsteady vortex lattice aerodynamics model with a plate finite element model. The aim is to optimize a flapping wing to maximize the thrust coefficient for micro air vehicle applications. Thus, the test case is not consistent with a fixed-wing aircraft. Walker et al. [15] did similar work for aeroelastic optimization of a flapping membrane wing for maximum thrust and propulsive efficiency. The aerodynamic forces were calculated using an analytical unsteady deformable thin airfoil theory.

# 1.2 Sensitivity methods

Accurate sensitivity analysis plays a fundamental role in achieving convergence for gradient-based optimization techniques. Various methods exist for evaluating sensitivities, including numerical methods (such as finite difference and complex step), analytical methods (including discrete analytical and continuum), hybrid methods (semi-analytical), and automatic differentiation methods. Among these, analytical methods are preferred due to their higher accuracy and lower computational time compared to numerical approaches. Analytical methods eliminate the need for convergence studies to determine an appropriate step size for numerical differentiation, as required by the Finite Difference Method (FDM), which is prone to truncation errors at large step sizes and roundoff errors at small ones [16, 17, 18]. Moreover, analytical methods do not rely on complex number operations such as the complex step method [19], making them more compatible with common commercial software that does not support complex numbers as shape parameters. Additionally, analytical methods do not require access to the analysis source code, a necessity for Automatic Differentiation (AD) [20, 21], allowing them to be implemented with black-box software. Discrete analytical methods are challenging to apply due to their reliance on mesh sensitivities [22]. However, recent developments made by the authors [23] have introduced an element-agnostic approach for calculating derivatives of stiffness, and mass matrices using primary analysis matrices and connectivity information. In this work, the same approach has been developed to differentiate damping matrices. The DLM is commonly employed to compute aerodynamic matrices, but their derivation through analytical means is not feasible, necessitating the use of FDM. Consequently, the developed method can be categorized as semi-analytical. It is worth noting that semi-analytical methods are known to be less accurate when dealing with shape sensitivity problems [24]. However, this characteristic has been assessed when structural matrices are numerically differentiated, while DLM aerodynamic matrices are here derived.

## 1.3 Semi-analytical differentiation

This work involves the discrete analytical differentiation of the flutter governing equations. Discrete analytical sensitivity methods have been formulated for complex eigenvalues in the case of nonviscously [25] and viscously damped [26] systems, asymmetric viscously damped systems [27], and to generally complex system matrices [28]. However, these methods were primarily developed for parameter design variables rather than shape design ones. Additionally, they were formulated for generic complex eigenvalue problems, whereas flutter equations are formulated in modal coordinates. To address these limitations, a novel methodology has been developed to handle flutter equations expressed in modal coordinates. This methodology requires the differentiation of the structural and aerodynamic matrices as well as real eigenvectors' derivatives. The differentiation of stiffness, mass, structural, and modal damping matrices is analytical and employs general and element-agnostic approaches that do not rely on specific knowledge of the structural parameters. Instead of explicitly calculating the differentiated matrices, existing primary analysis matrices and results are smartly employed to compute the matrix derivatives. Furthermore, the derivative of the primary modal analysis eigenvector matrix has been obtained using Nelson's sensitivity method [29], which is still discrete analytical. On the other hand, the differentiation of DLM aerodynamic matrices has been performed employing the finite difference method.

In the subsequent sections, a comprehensive description and mathematical treatment of the developed methodologies are provided. The Semi-Analytical Aeroelastic Sensitivity (SAAS) method is presented, which has been rigorously derived for both K- and PK-methods, widely employed in flutter analysis. The methodology has been assessed across various scenarios involving different stiffnesses, airspeeds, reduced frequencies, and types and amounts of structural damping.

# 2. Methodology

This chapter introduces the general discrete analytical formulation to calculate complex eigenvalue derivatives. The theory is then particularized for an aeroelastic shape design problem. A rigorous nonintrusive and element-agnostic methodology has been developed. The method requires primary analysis results such as eigenvalues and eigenvectors and the derivative of structural and aerodynamic matrices. Primary analysis matrices and results are used to calculate the required derivatives, resulting in an element-agnostic and computationally efficient approach.

## 2.1 K-method flutter equations

Several methods exist in the literature to solve flutter equations. In this section, the K-method is considered because of its easier demonstration, not requiring iterative eigenvalue calculations or aerodynamic matrices interpolations. Nevertheless, the sensitivity results can be useful to calculate flutter speed sensitivity in the same way. The philosophy behind the K-method is to inject the system with artificial damping (in the form of a structural damping term g) to push the system to the flutter point. The basic equation for modal flutter analysis by the K-method is [30]:

$$\[ -[M_{hh}]\omega^2 + i[B_{hh}]\omega + (1+ig)[K_{hh}] - \left(\frac{1}{2}\rho V^2\right)[Q_{hh}(M,k)] \] \{u_h\} = 0, \tag{1}$$

where:

- $[M_{hh}] = \text{modal mass matrix};$
- $[B_{hh}] = \text{modal damping matrix};$
- $[K_{hh}]$  = modal stiffness matrix, may be complex if actual structural damping  $g_s$  is employed, may be singular if rigid body modes are present;
- *M* = Mach number;
- $k = \frac{\omega \bar{c}}{2V} = \text{reduced frequency};$
- $\bar{c} = \text{reference length};$
- $[Q_{hh}(M,k)] =$  aerodynamic force matrix, which is a function of parameters M and k;
- $\omega = 2\pi f = \text{circular frequency};$
- *g* = artificial structural damping;
- ρ = fluid density;
- V = velocity:
- $\{u_h\}$  = modal amplitude vector.

The parameters k, V, and  $\omega$  are not independent from each other. For the K-method of solution, the aerodynamic term is converted to an equivalent aerodynamic mass:

$$\left[ -\left[ [M_{hh}] + \frac{\rho}{2} \left( \frac{\bar{c}}{2k} \right)^2 [Q_{hh}(M,k)] \right] \frac{\omega^2}{1 + ig} + [B_{hh}] \frac{i\omega}{\sqrt{1 + ig}} + [K_{hh}] \left\{ u_h \right\} = 0.$$
 (2)

The term involving  $[B_{hh}]$  in Eq. 2 has been multiplied by  $\sqrt{1+ig}$  for mathematical convenience. Eq. 2 is solved as an eigenvalue problem for a series of values for parameters M, k, and  $\rho$ . The complex eigenvalue is  $\omega^2/(1+ig)$ , which can be interpreted as real values of  $\omega$  and g. The velocity, V, is recovered from  $V=\omega\bar{c}/2k$ . Flutter occurs for values of M, k and  $\rho$  for which g=0. A different version of the equation is used within NASTRAN software. The equation is written as:

$$\left[ \left[ \left( \frac{2k}{\bar{c}} \right)^2 [M_{hh}] + \frac{\rho}{2} [Q_{hh}(M,k)] \right] \left( \frac{-V^2}{1+ig} \right) + \left( \frac{2k}{\bar{c}} \right) [B_{hh}] \frac{iV}{\sqrt{1+ig}} + [K_{hh}] \right] \{u_h\} = 0.$$
(3)

The new eigenvalue is therefore:

$$p^2 = \frac{-V^2}{1 + ig} \tag{4}$$

Eq. 4 may be written as:

$$p^{2} = V^{2} \frac{(1 - ig)}{1 + g^{2}} = a + ib, \tag{5}$$

so that:

$$g = -b/a, (6)$$

and

$$V = \sqrt{-\frac{(a^2 + b^2)}{a}}. (7)$$

The natural frequency can be also calculated since the reduced frequency is known:

$$f = \frac{kV}{\pi \bar{c}}. ag{8}$$

# 2.2 Differentiation of K-method equations

A generic complex eigenvalue problem is defined by the following equation:

$$([M]p^2 + [B]p + [K]) \{\phi\} = 0$$
(9)

The stiffness matrix [K] may be complex if the proper structural damping  $(g_s)$  is included in the model:  $[K] = (1 + ig_s)[K_{struct}]$ . Suppose that the system matrices in Eq. 9 are functions of a parameter b: in the current case a shape design variable. The derivatives of complex eigenvalues were obtained by Adhikari [31]. The following expression for the derivative of the j-th eigenvalue with respect to the design parameter b is obtained:

$$\frac{\partial p_j}{\partial b} = -\frac{\{\phi\}^T \left(p_j^2 [M'] + p_j [B'] + [K']\right) \{\phi\}}{\{\phi\}^T \left(2p_j [M] + [B]\right) \{\phi\}},\tag{10}$$

where the  $(\bullet)'$  symbol indicates the derivative with respect to b. Such an equation has been here extended to the aeroelastic model defined in modal coordinates (Eq. 3). However, the structural matrices can be analytically derived in the grid coordinated and not in the modal ones. Thus, the derivation of the modal stiffness  $([K_{hh}] = [\Phi_R]^T [K] [\Phi_R])$  or mass  $([M_{hh}] = [\Phi_R]^T [M] [\Phi_R])$  matrices also involves the derivative of the real eigenvector matrix  $[\Phi_R]$ :

$$[K'_{hh}] = \left[\Phi'_{R}\right]^{T} [K] \left[\Phi_{R}\right] + \left[\Phi_{R}\right]^{T} \left[K'\right] \left[\Phi_{R}\right] + \left[\Phi_{R}\right]^{T} [K] \left[\Phi'_{R}\right], \tag{11}$$

$$[M'_{hh}] = \left[\Phi'_R\right]^T [M] \left[\Phi_R\right] + \left[\Phi_R\right]^T \left[M'\right] \left[\Phi_R\right] + \left[\Phi_R\right]^T [M] \left[\Phi'_R\right]. \tag{12}$$

The real eigenvectors derivative ( $[\Phi'_R]$ ) can be calculated using Nelson's algorithm [29], described in detail in the following paragraphs. Such a method employs mass-normalized eigenvectors. As a consequence, the modal mass matrix is always the identity one ( $[M_{hh}] = [I]$ ) and does not depend on the design variable. Its derivative is therefore null:

$$[M'_{hh}] = [0]. (13)$$

Particularizing Eq. 10 for the K-method aeroelastic equation (Eq. 3) and substituting Eqs 11 and 13, the following general formula is obtained:

$$\frac{\partial p_{j}}{\partial b} = -\frac{\left\{u_{h,j}\right\}^{T} \left(p_{j}^{2} \frac{\rho}{2} [Q'_{hh}] + p_{j} \left(\frac{2k}{\bar{c}}\right) [B'_{hh}] + [\Phi'_{R}]^{T} [K] [\Phi_{R}] + \left[\Phi_{R}\right]^{T} [K] [\Phi'_{hh}] \right) \left\{u_{h,j}\right\}}{\left\{u_{h,j}\right\}^{T} \left(2p_{j} \left(\left(\frac{2k}{\bar{c}}\right)^{2} [M_{hh}] + \frac{\rho}{2} [Q_{hh}]\right) + \left(\frac{2k}{\bar{c}}\right) [B_{hh}]\right) \left\{u_{h,j}\right\}}.$$
(14)

Such an equation is of easy application and is far more convenient compared to the FDM, which involves several aeroelastic analyses to assess the step size. In particular, the developed SAAS method involves the following quantities:

- Primary analysis matrices, eigenvalues, and eigenvectors which are already calculated  $(p_j, \{u_{h,j}\}, [K], [\Phi_R], [M_{hh}], [B_{hh}], [Q_{hh}])$ .
- Known data and parameters  $(\rho, k, \bar{c})$ .
- Analytically and element-agnostically derived matrices ([K'],  $[B'_{hh}]$ ).
- Real eigenvector matrix derivative calculated with a discrete analytical (Nelson's) method ( $[\Phi'_R]$ ).
- Aerodynamic matrix differentiated with FDM ( $[Q'_{hh}]$ ).

# 2.3 PK-method flutter equations

The fundamental equation for modal flutter analysis by the PK-method is [30]:

$$\left[ [M_{hh}]p^2 + \left( [B_{hh}] - \frac{1}{4}\rho\bar{c}V[Q_{hh}^{\Im}]/k \right)p + \left( [K_{hh}] - \frac{1}{2}\rho V^2[Q_{hh}^{\Re}] \right) \right] \{u_h\} = 0,$$
(15)

where the new terms compared to the K-method are:

- $[Q_{hh}^3] = \text{modal aerodynamic damping matrix}$ , a function of Mach number, M, and reduced frequency, k;
- $[Q_{hh}^{\Re}] = \text{modal aerodynamic stiffness matrix}$ , a function of Mach number, M, and reduced frequency, k;
- $p = \omega(\gamma \pm i)$  eigenvalue;
- $\gamma$  = transient decay rate coefficient (The structural damping coefficient is  $g = 2\gamma$ ).

The Eq. 15 is written so that the matrix terms are all real:  $[Q_{hh}^{\Re}]$  and  $[Q_{hh}^{\Im}]$  are the real and imaginary parts of  $[Q_{hh}(M,k)]$ , respectively. The circular frequency and the reduced frequency are not independent of each other since  $k=\omega\bar{c}/2V$ , and furthermore, that:

$$k = \bar{c}/2V \cdot \Im(p). \tag{16}$$

Because of that, the eigenvalue problem is not closed, and it needs to be solved iteratively. This characteristic will make the eigenvalue derivative calculation iterative in the same way.

## 2.4 Differentiation of PK-method equations

The PK-method eigenvalue problem can be written in a general complex eigenvalue formulation (Eq. 9), and the Eq. 10 for the derivative of complex eigenvalues sensitivity applied. The relations 11 and 13, already found for the modal stiffness and mass matrix derivatives, can be still employed. However, the aerodynamic damping matrix depends on the reduced frequency, which in turn depends on the imaginary part of the eigenvalue through Eq. 16. As a consequence, the derivative of the term  $\left[\mathcal{Q}_{hh}^{3}\right]/k$  cannot be calculated since it depends on k', which in turn depends on p'. As in the case of the primary analysis, an iterative calculation is needed. A preliminary eigenvalue estimation can be obtained by assuming that the reduced frequency (k) is constant with the shape variable. The following equation for the PK-method eigenvalue calculation is thus obtained:

$$\frac{\left\{u_{h,j}\right\}^{T}\left(p_{j}\left(\left[B_{hh}'\right]-\frac{1}{4}\rho\bar{c}V\frac{\left[\left(Q_{hh}^{S}\right)'\right]}{k}\right)+\left[\Phi_{R}'\right]^{T}\left[K'\right]\left[\Phi_{R}\right]\left[\Phi_{R}\right]^{T}\left[K'\right]\left[\Phi_{R}\right]^{T}\left[K$$

Despite the previous formula being incorrect, a enough good estimation of the eigenvalue derivative is obtained. In particular, the damping term mainly affects the real part of the eigenvalue. As a

consequence, a very good estimation of  $\frac{\partial \Im(p_j)}{\partial b}$  is obtained which can be used to compute the reduced frequency derivative with respect to the shape:

$$k' = \frac{\bar{c}}{2V} \frac{\partial \Im(p_j)}{\partial b}.$$
 (18)

The estimation of k' allows the 'correct' computation of the derivative of the term  $\left[Q_{hh}^3\right]/k$ :

$$\frac{\partial}{\partial b} \left( \frac{\left[ Q_{hh}^{\Im} \right]}{k} \right) = \frac{\left[ \left( Q_{hh}^{\Im} \right)' \right] k - \left[ Q_{hh}^{\Im} \right] k'}{k^2} \tag{19}$$

The new estimation of the eigenvalue derivative can be calculated by means of Eq. 20.

$$\frac{\partial p_{j}}{\partial b} = -\frac{\left\{u_{h,j}\right\}^{T} \left(p_{j}\left(\left[B'_{hh}\right] - \frac{1}{4}\rho\bar{c}V\frac{\partial}{\partial b}\left(\frac{\left[Q_{hh}^{3}\right]}{k}\right)\right) + \left[\Phi_{R}^{2}\right]^{T}\left[K\right]\left[\Phi_{R}\right] + \left[\Phi_{R}\right]^{T}\left[K'\right]\left[\Phi_{R}\right] + \left[\Phi_{R}\right]^{T}\left[K\right]\left[\Phi_{R}^{2}\right] - \frac{1}{2}\rho V^{2}\left[\left(Q_{hh}^{\Re}\right)'\right]\right)\left\{u_{h,j}\right\}}{\left\{u_{h,j}\right\}^{T}\left(2p_{j}\left[M_{hh}\right] + \left[B_{hh}\right] - \frac{1}{4}\rho\bar{c}V\frac{\left[Q_{hh}^{3}\right]}{k}\right)\left\{u_{h,j}\right\}} \tag{20}$$

The new value of  $\frac{\partial p_j}{\partial b}$  allows a new estimation of the reduced frequency derivative (k'). The process can be iterated until two subsequent values of  $\frac{\partial p_j}{\partial b}$  are sufficiently close, based on the tolerance the user chooses. Typically, few iterations are needed due to the small influence of the shape parameter on the k' value.

#### 2.5 Derivative of structural matrices

The calculation of the derivatives of the stiffness, damping, and mass matrices with respect to shape variables is here discussed. The focus is on finding the eigenvalue derivatives with respect to the length of the beam  $L_b$ . Even when dealing with shape design variables, the derivative of the stiffness and mass matrices' elements is still with respect to a parameter: the length of the element. However, the derivative with respect to the whole beam length is needed instead of the beam element one. The derivative of a generic stiffness or mass matrix element  $A_{mn}$  with respect to the length of the beam can be written in terms of the length of the element ( $L_e$ ) by using the chain rule:

$$\frac{\partial A_{mn}}{\partial L_b} = \frac{\partial A_{mn}}{\partial L_e} \frac{\partial L_e}{\partial L_b}.$$
 (21)

The derivative  $\frac{\partial L_e}{\partial L_b}$  represents the elongation of the single beam element with respect to the elongation of the whole beam. It is easy to calculate using the design velocity  $\mathscr V$  formulation. Considering a generic finite element of a one-dimensional mesh connecting two nodes at x=a and x=b, the derivative is equal to:

$$\frac{\partial L_e}{\partial L_b} = \frac{\mathcal{V}_x|_{x=b} - \mathcal{V}_x|_{x=a}}{\mathcal{V}_x|_{x=L_b} - \mathcal{V}_x|_{x=0}}.$$
(22)

The focus can now be shifted to the derivative  $\frac{\partial A_{min}}{\partial L_e}$ . All the terms of the stiffness matrix of a generic beam element contain terms proportional to  $\frac{1}{L_e^\alpha}$ , with  $\alpha$  real parameter (i.e.  $\frac{EA}{L_e}$ ,  $\frac{6EI}{L_e^2}$  and  $\frac{12EI}{L_e^3}$ ). Also, the contribution of the mass matrix coming from the distributed mass depends on the element length. The derivative of this kind of function is elementary. In addition, the derivatives are calculated utilizing the primary analysis stiffness and mass matrix and the mesh connectivity, without explicitly building the derivative of the matrices. The methodology to differentiate the structural matrices has been already applied and validated by the authors for different eigenvalue sensitivity problems [23]. If structural damping is employed, no further derivations are necessary for the damping matrix. The derivative of the damping terms only requires the derivative of the stiffness matrix. However, if modal

damping is used in the model, the derivative of the modal damping matrix  $[B_{hh}]$  is needed. Its terms depend on known data and real eigenvalues derivative which is calculated anyway to apply Nelson's algorithm. In particular, Eq. 23 can be used to compute the modal damping matrix derivative. An element-agnostic approach can be still used employing the primary matrix. Considering the element of  $[B_{hh}]$  correspondent to the j-th mode, here indicated as  $B_{jj}$ , the derivative can be computed as follows:

$$\frac{\partial B_{jj}}{\partial b} = 2\zeta m_j \frac{\partial \omega_{n,j}}{\partial b} = 2\zeta m_j \omega_{n,j} \frac{\omega'_{n,j}}{\omega_{n,j}} = B_{jj} \frac{\omega'_{n,j}}{\omega_{n,j}}, \tag{23}$$

where  $\zeta$  is the critical damping coefficient, and  $\omega_{n,j}$  is the circular natural frequency of the j-th mode. The derivative of the circular frequency ( $\omega'_{n,j}$ ) is known since when applying Nelson's algorithm for deriving eigenvectors, real eigenvalues derivatives are also calculated, as discussed in the following paragraph.

# 2.6 Derivative of real eigenvector matrix

To calculate the derivative of the real eigenvector matrix, Nelson's algorithm for real eigenvalue problems can be used [29]. This method employs discrete analytical differentiation and requires the stiffness and mass matrices, along with their derivatives. Although traditionally applied to sizingtype design variables, recent work by the authors [32] demonstrates its applicability to shape design variables as well.

To apply Nelson's algorithm, it is necessary to calculate the derivative of the real eigenvalue. A primary modal analysis ( $[K]\phi_R = \lambda[M]\phi_R$ ) is always performed to obtain the modal parameters needed for subsequent aeroelastic calculations. If mass-normalized eigenvectors are used, the real eigenvalue derivative can be calculated using the following formula:

$$\lambda_{i}' = \{\phi_{R,j}\}^{T} ([K'] - \lambda_{j}[M']) \{\phi_{R,j}\},$$
(24)

where  $\{\phi_{R,j}\}$  is the j-th real eigenvector, and [K] and [M] are the structural matrices expressed in the grid set.

Defining the vector  $\{f\} \equiv \left(\lambda'_j[M] + \lambda_j[M'] - [K']\right) \{\phi_{R,j}\}$ , the following Nelson's algorithm can be used to calculate the j-th eigenvector derivative [33]:

- 1. Let  $[G] \equiv [K] \lambda_j[M]$  and assume  $\{\phi_{R,j}\} = (x_1, x_2, ..., x_n)^T$ .
- 2. Find k such that  $|x_k| = ||x_k||_{\infty} \equiv max_i|x_i|$ .
- 3. Replace the k-th row and column of [G] with zeros except for 1 on the k-th diagonal element. Call the result  $[\bar{G}]$ .
- 4. Replace the *k*-th element of  $\{f\}$  with zero. Call the result  $\{\bar{f}\}$ .
- 5. Solve  $[\bar{G}]\{v\} = \{\bar{f}\}.$
- 6. Compute  $c = -\{v\}^T[M]\{\phi_{R,j}\} 0.5\{\phi_{R,j}\}^T[M']\{\phi_{R,j}\}.$
- 7. Let  $\{\phi'_{R,i}\} = \{v\} + c\{\phi_{R,j}\}.$

Applying the previous algorithm for each eigenvector  $\{\phi_{R,j}\}$ , it is possible to obtain the eigenvectors' matrix derivative  $[\Phi'_R]$  required by the SAAS method.

# 2.7 Derivative of aerodynamic matrices

The DLM aerodynamic matrices calculation is not based on an original analytical theory. Thus, they cannot be differentiated by employing analytical methods. They are calculated by evaluating the lifting pressure distribution that generates the proper normalwash amplitude w at all the points located at 3/4 chord of each element [34]. In this work, the FDM has been employed to obtain the derivative of the sole aerodynamic matrix.

As mentioned earlier, the aerodynamic matrices are dependent on the reduced frequency. When using the semi-analytical differentiation in the K-method case, the reduced frequency is fixed and only a single aerodynamic matrix needs to be differentiated. In contrast, each PK-method eigenvalue corresponds to a different reduced frequency. There is therefore a need to consider multiple aerodynamic matrices and then perform interpolations. In particular, the interpolation must be done in a specific way when performing finite differences. The PK-method operates at a constant airspeed, and when a geometric shape variable (b) is altered, the eigenvalue associated with the same airspeed corresponds to a different reduced frequency. Consequently, the aerodynamic matrices corresponding to  $b + \Delta b$  and  $b - \Delta b$  must be interpolated at the new reduced frequencies. Calculating all matrices at the nominal k value would introduce errors. When considering a general single eigenvalue p characterized by a specific reduced frequency k, the forward and backward derivatives must be computed for each step size  $\Delta b$  at the corresponding reduced frequencies  $k_{b+\Delta b} = k(b+\Delta b)$  and  $k_{b-\Delta b} = k(b-\Delta b)$ . Ignoring the Mach number dependence for the sake of simplicity, it is known that the aerodynamic matrix is dependent on the reduced frequency and the shape design variable b due to its influence on the aerodynamic panel dimensions ( $[Q_{bh}(k,b)]$ ). Employing equations 25 and 26, the forward and backward derivatives of each term of the aerodynamic matrix ( $[Q_{hh}(k,b)]_{ii}$ ) can be calculated, respectively.

$$\frac{\partial [Q_{hh}(k,b)]_{ij}}{\partial b}\bigg|_{FWD} \simeq \frac{[Q_{hh}(k_{b+\Delta b},b+\Delta b)]_{ij} - [Q_{hh}(k,b)]_{ij}}{\Delta b}$$
(25)

$$\frac{\partial [Q_{hh}(k,b)]_{ij}}{\partial b}\bigg|_{BWD} \simeq \frac{[Q_{hh}(k,b)]_{ij} - [Q_{hh}(k_{b-\Delta b},b-\Delta b)]_{ij}}{\Delta b} \tag{26}$$

In addition, the convergence of finite differences should be studied separately for each element instead of the overall matrix. In general, the optimal step size can be different for each element of the matrix. In the end, the overall differentiated matrix  $[Q'_{hh}]$  will contain the derivatives of the various elements of  $[Q_{hh}]$ , each calculated in its optimal step size employing the central difference scheme. More practically, the finite differences of the aerodynamic matrices are calculated at the same values of the reduced frequencies as the primary analysis  $k_r = k_1, k_2, \ldots, k_r$  and for each step size. The aerodynamic matrices  $[Q_{hh}(k_r,b)]$  are already available from the primary analysis, while the  $[Q_{hh}(k_r,b-\Delta b)]$  and  $[Q_{hh}(k_r,b+\Delta b)]$  ones must be computed. They are employed to calculate the  $[Q_{hh}(k_{b+\Delta b},b+\Delta b)]_{ij}$  and  $[Q_{hh}(k_{b-\Delta b},b-\Delta b)]_{ij}$  values necessary to apply Eqs 25 and 26. Convergence studies are performed to find the best step size and finally, the central difference scheme is applied for the final derivative estimation:

$$\frac{\partial [Q_{hh}(k,b)]_{ij}}{\partial b}\bigg|_{C} \simeq \frac{[Q_{hh}(k_{b+\Delta b},b+\Delta b)]_{ij} - [Q_{hh}(k_{b-\Delta b},b-\Delta b)]_{ij}}{2\Delta b}.$$
(27)

## 3. Applications and results

In this section, the SAAS method is applied to a cantilever rectangular wing, with its length considered as a shape design variable. The effectiveness of this approach has been evaluated for both K- and PK-methods under various conditions. Specifically, the stiffness, reduced frequency, airspeed, and structural or modal damping have been systematically varied to validate the methodology across a range of scenarios.

## 3.1 Aeroelastic model

A cantilever wing aeroelastic model has been considered to validate the sensitivity methods. The wing has a rectangular shape with a  $1\,\mathrm{m}$  chord and a midspan of  $4.5\,\mathrm{m}$ . A stick-beam structural model has been developed (Figure 1). In order to validate the method in a general condition, a variable mesh size has been employed. Both continuous (density) and point masses have been employed to model the inertia. It makes more tricky the differentiation of the mass matrix since the components due to density vary with shape, while point masses do not. DLM has been employed for the aerodynamic model (Figure 2). The structural and aerodynamic degrees of freedom have been connected through a linear spline. This aeroelastic model closely aligns with the standard models utilized during the

design and optimization phases, which are the focus of this work. Generally, beam-like models are used to simulate the overall stiffness characteristic of the wing, and point masses are used to simulate the non-structural mass.

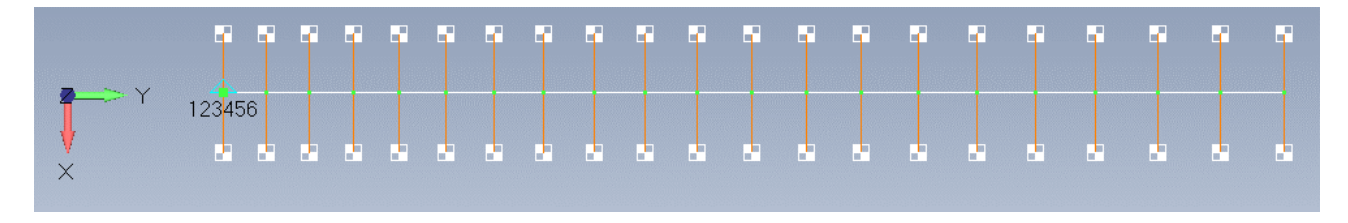


Figure 1 – Cantilever wing stick-beam structural model.

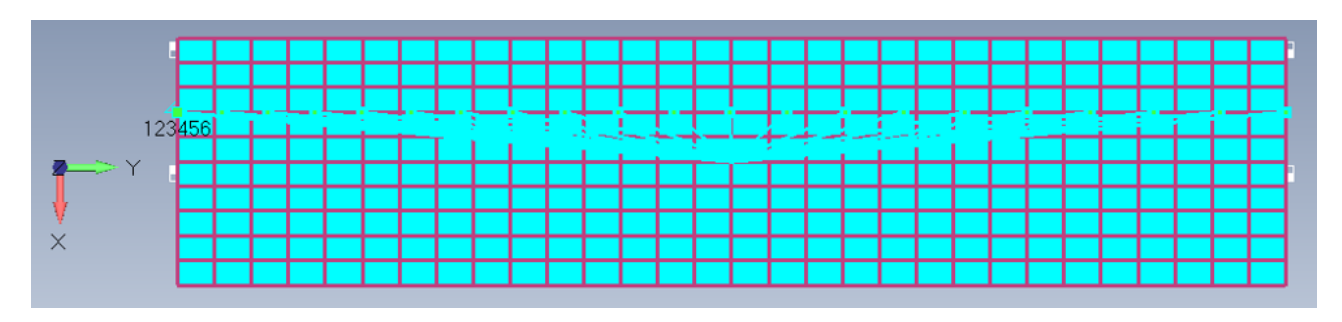


Figure 2 - Cantilever wing aerodynamic panel and spline.

# 3.2 Validation of the discrete analytical differentiation in modal coordinates

Before incorporating the derivatives of the aerodynamic matrices into the model, it is essential to assess the discrete analytical differentiation in modal coordinates. For this purpose, the structure of the cantilever wing model has been considered, with its length treated as a shape design variable. The first eight eigensensitivities have been calculated using the well-established and validated Nelson's formula (Eq. 24), along with the proposed methodology in modal coordinates. By applying Nelson's equation to the matrices and eigenvectors expressed in the modal coordinates instead of the grid set and taking advantage of the Eqs. 11 and 13, the following formula is obtained:

$$\lambda_{j}' = \left\{\phi_{M,j}\right\}^{T} \left(\left[K_{hh}'\right] - \lambda_{j}\left[M_{hh}'\right]\right) \left\{\phi_{M,j}\right\}$$

$$= \left\{\phi_{M,j}\right\}^{T} \left(\left[\Phi_{R}'\right]^{T}\left[K\right]\left[\Phi_{R}\right] + \left[\Phi_{R}\right]^{T}\left[K'\right]\left[\Phi_{R}\right] + \left[\Phi_{R}\right]^{T}\left[K\right]\left[\Phi_{R}'\right]\right) \left\{\phi_{M,j}\right\},$$
(28)

where  $\{\phi_{M,j}\}$  represents the j-th modal (real) eigenvector. The first eight natural frequencies of the wing are presented in Table 1. Additionally, the derivative of the natural frequency with respect to the wing length, evaluated using Nelson's method in both the grid and modal coordinates, is provided. The reference values are obtained using the NASTRAN Design Sensitivity and Optimization solution (SOL 200) [4]. An excellent correspondence between the results obtained in the grid and modal sets and the reference values has been obtained. It validates the novel discrete analytical differentiation in the modal coordinates introduced in this paper. Furthermore, it confirms the consistency of the derivative of the eigenvector matrix  $[\Phi_R']$ , which is calculated using Nelson's algorithm.

Table 1 – Natural frequencies and their derivative with respect to the wing length. Comparison between the differentiation in the grid and modal set with respect to NASTRAN SOL 200 reference values.

| Mode | f     | Mode                    | Natural frequency derivative, $f'$ (Hz/mm) |             |             |
|------|-------|-------------------------|--|-------------|-------------|
| ID   | (Hz)  | description             | Grid set                                   | Modal set   | SOL 200     |
| 1    | 5.636 | First vertical bending  | -2.2914E-03                                | -2.2915E-03 | -2.2915E-03 |
| 2    | 22.49 | First fore-and-aft      | -9.1108E-03                                | -9.1116E-03 | -9.1118E-03 |
| 3    | 34.74 | Second vertical bending | -1.4064E-02                                | -1.4064E-02 | -1.4064E-02 |
| 4    | 67.91 | First torsion           | -7.5457E-03                                | -7.5457E-03 | -7.5457E-03 |
| 5    | 96.55 | Third vertical bending  | -3.9039E-02                                | -3.9039E-02 | -3.9039E-02 |
| 6    | 136.7 | Second fore-and-aft     | -5.4073E-02                                | -5.4074E-02 | -5.4074E-02 |
| 7    | 188.5 | Fourth vertical bending | -7.6213E-02                                | -7.6213E-02 | -7.6213E-02 |
| 8    | 195.8 | Second torsion          | -2.1759E-02                                | -2.1759E-02 | -2.1759E-02 |

#### 3.3 K-method solution results

The first application involves calculating the derivative of all flutter eigenvalues with respect to the length of the beam. To also validate the differentiation of the modal damping matrix, a critical damping coefficient of  $\zeta=0.05$  is introduced. A reduced frequency of k=1.0 is selected. Table 2 provides the first eight flutter eigenvalues, along with their corresponding natural frequencies and damping coefficients. The second and sixth mode shapes are fore-and-aft ones and are poorly affected by aerodynamics. Consequently, the damping coefficient is essentially equal to the structural one ( $g\approx 2\zeta$ ).

Table 2 – Flutter eigenvalues with corresponding natural frequencies and damping coefficients: nominal stiffness, k = 1.0, structural damping  $\zeta = 0.05$ .

| Mode | Flutter                 | Natural             | Damping        |
|------|-------------------------|---------------------|----------------|
| ID   | eigenvalue, $p$         | frequency, $f$ (Hz) | coefficient, g |
| 1    | -9.3327e+2 + 1.7629e+4i | 5.635               | -1.061e-1      |
| 2    | -3.5326e+3 + 7.0563e+4i | 22.55               | -1.004e-1      |
| 3    | -5.7276e+3 + 1.0869e+5i | 34.74               | -1.060e-1      |
| 4    | -1.6681e+4 + 2.0859e+5i | 67.04               | -1.610e-1      |
| 5    | -1.5779e+4 + 3.0212e+5i | 96.56               | -1.047e-1      |
| 6    | -2.1478e+4 + 4.2902e+5i | 137.1               | -1.004e-1      |
| 7    | -3.0547e+4 + 5.8990e+5i | 188.5               | -1.038e-1      |
| 8    | -4.5509e+4 + 6.0306e+5i | 193.6               | -1.518e-1      |

The eigenvalues have been differentiated with respect to the length of the wing, and the results are compared to the FDM ones calculated at the optimal step size. Finite differences require performing the complete flutter analysis multiple times for both backward and forward derivatives to determine the optimal step size. Once the optimal step is found, the derivative of the reference eigenvalues is calculated using the central difference scheme. In contrast, the SAAS method offers a more convenient procedure. It involves a formula with elements that are either already known or can be calculated analytically using simple operations. Only the aerodynamic terms are derived using FDM. The results of the differentiation are summarized in Table 3. A good correspondence has been achieved for all the considered modes, both in terms of the real and imaginary parts of the eigenvalues. However, it should be noted that the  $4^{th}$  and  $8^{th}$  modes, which are torsional modes, exhibit relatively larger errors, particularly in the real part, which represents damping. This can be attributed to the higher sensitivity of these eigenvalues to aerodynamic terms, which are derived using FDM and therefore have lower accuracy. The obtained eigensensitivities enable the calculation of derivatives for the natural frequencies and damping coefficients, providing valuable guidelines for aeroelastic shape design. Moreover, these accurate and efficient derivatives can be utilized in gradient-based optimization techniques. Importantly, the procedure does not require access to the software source code and is independent

Table 3 – Flutter eigenvalues derivative with respect to the wing length. Comparison between the semi-analytical method and FDM results, k = 1.0, structural damping  $\zeta = 0.05$ .

| Mode | FDM               | Semi-analytical   | $\Re(p')$ error | $\Im(p')$ error |
|------|-------------------|-------------------|-----------------|-----------------|
| ID   | derivative $(p')$ | derivative $(p')$ | (%)             | (%)             |
| 1    | 0.37219 -7.1737i  | 0.37217 -7.1737i  | -0.00537        | 0.00000         |
| 2    | 1.43127 -28.5900i | 1.43131 -28.5890i | 0.00279         | 0.00350         |
| 3    | 2.27494 -44.0370i | 2.27397 -44.0371i | -0.04264        | -0.00023        |
| 4    | 0.43050 -24.2580i | 0.42292 -24.2294i | -1.76074        | 0.11790         |
| 5    | 6.25120 -122.280i | 6.24864 -122.281i | -0.04095        | -0.00082        |
| 6    | 8.49380 -169.665i | 8.49347 -169.665i | -0.00389        | 0.00000         |
| 7    | 12.1126 -238.810i | 12.1134 -238.803i | 0.00660         | 0.00293         |
| 8    | 1.22230 -69.9030i | 1.21075 -69.8579i | -0.94494        | 0.06452         |

of the properties of the structural elements, making it highly suitable for practical applications.

To comprehensively assess the semi-analytical method under various conditions, variations in the reduced frequency, stiffness, type, and amount of structural damping have been conducted. The results of the sensitivity analysis are presented in Table 4. For brevity, only one eigenvalue for each type of mode shape (vertical bending, fore-and-aft, and torsional) has been considered. The correspondence of the remaining modes is analogous within each mode shape category. Notably, the error in the imaginary part of the eigenvalues remains consistently low across all scenarios. This holds true even when the wing stiffness is significantly reduced, resulting in substantial variations in natural frequencies and the occurrence of instabilities with changes in airspeed.

When no structural damping is employed, the real part of the fore-and-aft eigenvalues is essentially zero, rendering the derivative undefined. However, when structural damping is incorporated, the derivative of the real part of the eigenvalue depends solely on the structural matrices, which are differentiated analytically. Consequently, the error in the real part is extremely low. The bending mode (1) exhibits a high level of correspondence across the various scenarios for the real part of the eigenvalue.

The SAAS approach has been successfully utilized to compute shape design derivatives for aeroelastic problems using the K-method of solution. The method has demonstrated its effectiveness across various scenarios, involving parameter variations such as stiffness, reduced frequency, and different types and levels of damping. Notably, the error is low across the various scenarios and is further reduced when the derivative is only due to analytically differentiated matrices (mode 6). It suggests a further improvement in accuracy if the aerodynamic matrices are more efficiently derived.

## 3.4 PK-method solution results

In this chapter, the semi-analytical differentiation has been applied and validated for the PK-method of solution. Initially, the method was applied to a case with nominal stiffness, along with the inclusion of a structural damping coefficient of  $\zeta=0.05$ . Table 5 provides a summary of the first eight flutter eigenvalues, including their corresponding flutter frequencies and damping coefficients. It is worth noting that the damping of the fore-and-aft modes is nearly equal to the structural damping, being almost unaffected by aerodynamic loads.

The semi-analytical derivatives were compared to finite differences calculated at the optimal step size (Table 6). PK-method of solution requires an iterative eigenvalue calculation since the eigenvalue depends on the reduced frequency. However, the sensitivity of the reduced frequency, k, to changes in shape is small. Therefore, only a few iterations are required for the differentiated problem. As the flutter eigenvalues corresponding to the same airspeed are associated with different reduced frequencies, equations 17 and 20 utilize distinct aerodynamic matrix derivatives for each mode. Thus, a different formula must be utilized for each mode, while the same formula can be used for all modes in the K-method case.

A strong correspondence has been achieved for the imaginary part of the eigenvalue derivative. For what concerns the real part, the correlation is good for bending modes (1, 3, 5, 7). Fore-and-aft

Table 4 – Derivative of three representative flutter eigenvalues with respect to the wing length. Comparison between the semi-analytical method and FDM results, K-method.

| Mode  | FDM                          | Semi-analytical               | $\Re(p')$ error | $\Im(p')$ error |  |
|---|------------------------------|-------------------------------|-----------------|-----------------|--|
| ID  |                              | derivative $(p')$             | (%)             | (%)             |  |
| Nominal stiffness, $k = 0.5$ , no structural damping        |                              |                               |                 |                 |  |
| 1   | 0.05889 -14.3691i            | 0.05891 -14.3692i             | 0.03396         | -0.00070        |  |
| 6   | 0.00000 -339.754i            | 0.00000 -339.754i             | -               | 0.00000         |  |
| 8   | -8.19420 -143.170i           | -8.19106 -142.361i            | -0.03832        | 0.56506         |  |
| Nomina  | al stiffness, $k = 1.0$ , no | structural damping            |                 |                 |  |
| 1   | 0.01379 -7.1840i             | 0.01377 -7.1840i              | -0.14503        | 0.00000         |  |
| 6   | 0.00000 -169.8770i           | 0.00000 -169.877i             | -               | 0.00000         |  |
| 8   | -2.35010 -69.7700i           | -2.36004 -69.724i             | 0.42296         | 0.06593         |  |
| Nomina  | al stiffness, $k = 5.0$ , no | structural damping            |                 |                 |  |
| 1   | 0.000291 -1.4376i            | 0.000290 -1.4376i             | 0.34364         | 0.00000         |  |
| 6   | 0.000000 -33.9754i           | 0.000000 -33.9754i            | -               | 0.00000         |  |
| 8   | -0.09852 -13.8480i           | -0.098650 -13.8495i           | -0.13195        | -0.01083        |  |
| Reduce  |                              | (GJ/30), k = 1.0,  no struct  |                 |                 |  |
| 1   | 0.00252 -1.3116              | 0.00251 -1.3116 i             | -0.39683        | 0.00000         |  |
| 6   | 0.00000 -31.0151             | 0.00000 -31.0150 i            | -               | -0.00032        |  |
| 8   | -0.42908 -12.7390            | -0.43088 -12.7300 i           | 0.41950         | 0.07222         |  |
|   |                              | d GJ/100), $k = 1.0$ , no str |                 |                 |  |
| 1   | 0.001379 -0.7184i            | 0.001379 -0.7184i             | 0.00000         | 0.00000         |  |
| 6   | 0.000000 -16.9877i           | 0.000000 -16.9877i            | -               | 0.00000         |  |
| 8   | -0.235010 -6.9770i           | -0.236000 -6.9724i            | 0.42126         | 0.06593         |  |
|   |                              | uctural damping $g_s = 0.04$  |                 |                 |  |
| 1   | 0.15744 -7.1851i             | 0.15742 -7.1852i              | -0.01270        | -0.00139        |  |
| 6   | 3.39685 -169.911i            | 3.39687 -169.911i             | 0.00059         | 0.00000         |  |
| 8   | -0.95550 -69.8300i           | -0.96631 -69.7849i            | 1.13134         | 0.06459         |  |
|   |                              | uctural damping $g_s = 0.10$  |                 |                 |  |
| 1   | 0.37256 -7.1923i             |                               | -0.00537        | 0.00000         |  |
| 6   | 8.48320 -170.088i            |                               | 0.00106         | 0.00000         |  |
| 8   | 1.13100 -69.9740i            | 1.11887 -69.9290i             | -1.07250        | 0.06502         |  |
| Nomina  |                              | uctural damping $g_s = 0.20$  |                 |                 |  |
| 1   | 0.72872 -7.2181i             | 0.72871 -7.2181i              | -0.00137        | 0.00000         |  |
| 6   | 16.9042 -170.716i            | 16.9042 -170.716i             | 0.00000         | 0.00000         |  |
| 8   | 4.58090 -70.3480i            | 4.56661 -70.3041i             | -0.31195        | 0.06240         |  |
|   | al stiffness, $k = 1.0$ , mo |                               |                 |                 |  |
| 1   | 0.157164 -7.18205i           | 0.157142 -7.18203i            | -0.01400        | 0.00028         |  |
| 6   | 3.397570 -169.845i           | 3.397586 -169.843i            | 0.00047         | 0.00118         |  |
| 8   | -0.922800 -69.8480i          | -0.933590 -69.8000i           | 1.16927         | 0.06872         |  |
| Nominal stiffness, $k = 1.0$ , modal damping $\zeta = 0.05$ |                              |                               |                 |                 |  |
| 1   | 0.37219 -7.1737i             | 0.37217 -7.1737i              | -0.00537        | 0.00000         |  |
| 6   | 8.49380 -169.665i            | 8.49347 -169.665i             | -0.00389        | 0.00000         |  |
| 8   | 1.22230 -69.9030i            | 1.21075 -69.8579i             | -0.94494        | 0.06452         |  |
| Nominal stiffness, $k = 1.0$ , modal damping $\zeta = 0.10$ |                              |                               |                 |                 |  |
| 1   | 0.73050 -7.1455i             | 0.73043 -7.1454i              | -0.00958        | 0.00140         |  |
| 6   | 16.9878 -169.025i            | 16.9879 -169.026i             | 0.00059         | -0.00059        |  |
| 8   | 4.81110 -69.8625i            | 4.79754 -69.8078i             | -0.28185        | 0.07830         |  |
|   |                              |                               | 5.25.00         |                 |  |

modes (2 and 6) exhibit a very good correspondence, as they are almost independent of the aerodynamic loads, which are differentiated using FDM. Torsional modes have a stronger dependence on the aerodynamic loads, resulting in relatively larger errors.

Table 5 – Flutter eigenvalues with corresponding natural frequencies and damping coefficients calculated with PK-method: nominal stiffness,  $V = 30 \, \mathrm{m/s}$ , modal damping  $\zeta = 0.05$ .

| Mode | Flutter                 | Natural             | Damping          |
|------|-------------------------|---------------------|------------------|
| ID   | eigenvalue, $p$         | frequency, $f$ (Hz) | coefficient, $g$ |
| 1    | -3.7352e+0 + 3.5128e+1i | 5.613               | -1.114e-1        |
| 2    | -1.4130e+1 + 1.4060e+2i | 22.46               | -1.001e-1        |
| 3    | -2.1958e+1 + 2.1661e+2i | 34.61               | -1.016e-1        |
| 4    | -4.3901e+1 + 4.2084e+2i | 67.24               | -1.068e-1        |
| 5    | -6.0699e+1 + 6.0278e+2i | 96.30               | -1.004e-1        |
| 6    | -8.5912e+1 + 8.5482e+2i | 136.6               | -1.001e-1        |
| 7    | -1.1841e+2 + 1.1778e+3i | 188.2               | -1.001e-1        |
| 8    | -1.2301e+2 + 1.2220e+3i | 195.2               | -1.002e-1        |

Table 6 – Flutter eigenvalues derivative with respect to the wing length, PK-method. Comparison between the semi-analytical method and FDM results: nominal stiffness,  $V=30\,\mathrm{m/s}$ , modal damping  $\zeta=0.05$ .

| Mode | FDM                 | Semi-analytical     | $\Re(p')$ error | $\Im(p')$ error |
|------|---------------------|---------------------|-----------------|-----------------|
| ID   | derivative $(p')$   | derivative $(p')$   | (%)             | (%)             |
| 1    | 0.000681 -0.014342i | 0.000681 -0.014345i | -0.01175        | -0.02092        |
| 2    | 0.002863 -0.057178i | 0.002863 -0.057150i | -0.00349        | 0.04897         |
| 3    | 0.004374 -0.088169i | 0.004375 -0.088150i | 0.02515         | 0.02155         |
| 4    | 0.001849 -0.048263i | 0.001865 -0.048300i | 0.84352         | -0.07666        |
| 5    | 0.012220 -0.24521i  | 0.012220 -0.24525i  | 0.00000         | -0.01631        |
| 6    | 0.016987 -0.33933i  | 0.016985 -0.33935i  | -0.01177        | -0.00589        |
| 7    | 0.023931 -0.47876i  | 0.023930 -0.47900i  | -0.00418        | -0.05013        |
| 8    | 0.006767 -0.13801i  | 0.006770 -0.13800i  | 0.04433         | 0.00725         |

The semi-analytical method has been applied to a wide range of scenarios, including different air-speeds, stiffnesses, and types and amounts of structural damping. The error relative to the imaginary part of the eigenvalue derivative remains consistently low across these scenarios. The representative bending mode demonstrates good correspondence for the real part as well. While the derivative of the fore-and-aft eigenvalues is undefined in undamped cases, its correspondence is very good in damped cases, as it depends solely on analytically differentiated structural matrices. Similar to the K-method, the torsional mode exhibits larger errors in the real part due to its increased dependence on numerically differentiated aerodynamic matrices. However, the error decreases in damped cases, as a portion of the damping derivative relies on analytically differentiated structural matrices.

The SAAS method has been successfully employed to compute shape design derivatives for aeroelastic problems using the PK-method of solution. The sensitivity method has been assessed across various scenarios, involving parameter variations such as stiffness, airspeed, and different types and amounts of structural damping. Contrary to the K-method, the PK one is the most diffusely employed in the flutter analysis due to its higher accuracy and usefulness of the output results, which are explicitly provided for each airspeed. The PK semi-analytical sensitivity method can be thus applied to general aeroelastic shape optimization problems.

## 4. Conclusion

This work presented innovative semi-analytical methods for calculating shape design derivatives of aeroelastic problems. Existing methods allow for the derivation of complex eigenvalues when the problem is formulated in grid coordinates. A novel methodology has been developed to differentiate flutter equations in the modal coordinates, which involves the derivative of the real eigenvector matrix. The derivative of the eigenvectors has been calculated using a discrete analytical approach. Furthermore, an element-agnostic approach has been developed to differentiate the mass, damping, and stiffness matrices with respect to the shape. The semi-analytical sensitivity method has been as-

Table 7 – Derivative of three representative flutter eigenvalues with respect to the wing length. Comparison between the semi-analytical method and FDM results, PK method.

| Mode   | FDM  | Semi-analytical                             | $\Re(p')$ error | $\Im(p')$ error |  |
|--------|--|---|-----------------|-----------------|--|
| ID     | derivative $(p')$  | derivative $(p')$                           | (%)             | · (%)           |  |
| Nomina | al stiffness, $V = 30 \mathrm{m/s}$ , no                           | structural damping                          |                 | · · ·           |  |
| 1      | -3.9324e-5 -0.014358i  | -3.9350e-5 -0.014358i                       | 0.06612         | 0.00000         |  |
| 6      | 0.00000 -0.339750i   | 0.00000 -0.339750i                          | -               | 0.00000         |  |
| 8      | -6.8553e-5 -0.138180i  | -6.7195e-5 -0.138000i                       | -1.98095        | 0.13026         |  |
| Nomina | al stiffness, $V = 100 \mathrm{m/s}$ , n                           | o structural damping                        |                 |                 |  |
| 1      | -1.4088e-4 -0.014390i  | -1.4083e-4 -0.014363i                       | -0.03904        | 0.18763         |  |
| 6      | 0.00000 -0.33975i  | 0.00000 -0.33975i                           | -               | 0.00000         |  |
| 8      | -1.4512e-3 -0.13917i   | -1.4273e-3 -0.139000i                       | -1.64691        | 0.12215         |  |
| Reduce | ed stiffness ( $EI/30$ and $GJ$                                    | $V/30$ ), $V = 30 \mathrm{m/s}$ , no struct | ural damping    |                 |  |
| 1      | -4.8492e-5 -0.002637i  | -4.7950e-5 -0.002635i                       | -1.11771        | 0.07586         |  |
| 6      | 0.00000 -0.062030i   | 0.00000 -0.062050i                          | -               | -0.03224        |  |
| 8      | -1.6278e-3 -0.028749i  | -1.6250e-3 -0.028800i                       | -0.17201        | -0.17740        |  |
| Reduce | ed stiffness ( $EI/100$ and $C$                                    | $GJ/100$ ), $V = 30\mathrm{m/s}$ , no stru  | ıctural damping |                 |  |
| 1      | -5.2335e-5 -1.5108e-3i   | -5.1725e-5 -1.5123e-3i                      | -1.16557        | -0.09929        |  |
| 6      | 0.00000 -3.3975e-2i  | 0.00000 -3.3975e-2i                         | -               | 0.00000         |  |
| 8      | -4.4948e-4 -1.3865e-2i   | -4.4520e-4 -1.3925e-2i                      | -0.95221        | -0.43274        |  |
| Nomina | al stiffness, $V = 30 \mathrm{m/s}$ , sti                          | ructural damping $g_s = 0.04$               |                 |                 |  |
| 1      | 0.000249 -0.014356i  | 0.000249 -0.014355i                         | 0.00804         | 0.00697         |  |
| 6      | 0.006795 -0.33969i   | 0.006795 -0.33970i                          | 0.00000         | -0.00294        |  |
| 8      | 0.002666 -0.13815i   | 0.002665 -0.13825i                          | -0.02626        | -0.07239        |  |
| Nomina | al stiffness, $V = 30 \mathrm{m/s}$ , sti                          | ructural damping $g_s = 0.10$               |                 |                 |  |
| 1      | 0.000681 -0.014342i  | 0.000681 -0.014345i                         | -0.01175        | -0.02092        |  |
| 6      | 0.016985 -0.33935i   | 0.016987 -0.339330i                         | 0.01153         | 0.00599         |  |
| 8      | 0.006770 -0.13800i   | 0.006767 -0.138012i                         | -0.04434        | -0.00896        |  |
| Nomina | al stiffness, $V = 30 \mathrm{m/s}$ , sti                          | ructural damping $g_s = 0.20$               |                 |                 |  |
| 1      | 0.001401 -0.014289i  | 0.001401 -0.014290i                         | 0.00000         | -0.00700        |  |
| 6      | 0.033976 -0.33805i   | 0.033980 -0.33805i                          | 0.01177         | 0.00000         |  |
| 8      | 0.013602 -0.13751i   | 0.013600 -0.13750i                          | -0.01470        | 0.00727         |  |
| Nomina | al stiffness, $V = 30 \mathrm{m/s}$ , m                            |   |                 |                 |  |
| 1      | 0.000249 -0.014356i  | 0.000249 -0.014355i                         | 0.00804         | 0.00697         |  |
| 6      | 0.006795 -0.33969i   | 0.006795 -0.33970i                          | 0.00000         | -0.00294        |  |
| 8      | 0.002666 -0.13815i   | 0.002665 -0.13825i                          | -0.02626        | -0.07239        |  |
| Nomina | al stiffness, $V = 30 \mathrm{m/s}$ , m                            |   |                 |                 |  |
| 1      | 0.000681 -0.014342i  | 0.000681 -0.014345i                         | -0.01175        | -0.02092        |  |
| 6      | 0.016987 -0.33933i   | 0.016985 -0.33935i                          | -0.01177        | -0.00589        |  |
| 8      | 0.006767 -0.13801i   | 0.006770 -0.13800i                          | 0.04433         | 0.00725         |  |
| Nomina | Nominal stiffness, $V=30\mathrm{m/s}$ , modal damping $\zeta=0.10$ |   |                 |                 |  |
| 1      | 0.001401 -0.014289i  | 0.001401 -0.01429i                          | 0.00000         | -0.00700        |  |
| 6      | 0.033976 -0.33805i   | 0.033980 -0.33805i                          | 0.01177         | 0.00000         |  |
| 8      | 0.013602 -0.13751i   | 0.013600 -0.13750i                          | -0.01470        | 0.00727         |  |

sessed in a wide range of scenarios, including various reduced frequencies, airspeeds, stiffnesses, types, and amounts of structural damping. The semi-analytical method has been developed for both the K-method and PK-method of flutter solution, making it practical for aeroelastic shape optimization of real airplanes. The accuracy of the method can be further improved by using more precise methods to differentiate the aerodynamic matrices, which is deferred to future works. The developed tool is a valid method to optimize aircraft shape leading the way to a more accurate and efficient aeroelastic tailored design.

## 5. Contact Author Email Address

Corresponding author email address: giuseppemaurizio.gagliardi@unina.it

# 6. Copyright Statement

The authors confirm that they, and/or their company or organization, hold copyright on all the original material included in this paper. The authors also confirm that they have obtained permission, from the copyright holder of any third-party material included in this paper, to publish it as part of their paper. The authors confirm that they give permission or have obtained permission from the copyright holder of this paper, for the publication and distribution of this paper as part of the ICAS proceedings or as individual off-prints from the proceedings.

## References

- [1] Yang C, Yang Y and Wu Z. Shape sensitivity analysis of flutter characteristics of a low aspect ratio supersonic wing using analytical method. *Science China Technological Sciences*, Springer, Vol. 55, pp 3370-3377, 2012.
- [2] Liu Y and Kapania R K. Modal response of trapezoidal wing structures using second-order shape sensitivities. *AIAA journal*, Vol. 38, pp 732-735, 2000.
- [3] Demasi L. Introduction to Unsteady Aerodynamics and Dynamic Aeroelasticity. 1st edition, Springer Nature Switzerland, 2024.
- [4] MSC Nastran. Design Sensitivity and Optimization User's Guide. *The Mac-Neal Schwendler Corporation*, 2022.
- [5] Kulkarni M D, Canfield R A and Patil M. Continuum sensitivity analysis for aeroelastic shape optimization. *57th AIAA/ASCE/AHS/ASC Structures, Structural Dynamics, and Materials Conference*, San Diego, California, pp 1177, 2016.
- [6] Palacios F and others. Stanford university unstructured (SU2): an open-source integrated computational environment for multi-physics simulation and design. *51st AIAA aerospace sciences meeting including the new horizons forum and aerospace exposition*, Grapevine, Texas, pp 287, 2013.
- [7] Liu S and Canfield R. Continuum shape sensitivity for nonlinear transient aeroelastic gust response. 52nd AIAA/ASME/ASCE/AHS/ASC Structures, Structural Dynamics and Materials Conference, Denver, Colorado, pp 1971, 2011.
- [8] Cross D and Canfield R. Continuum shape sensitivity with spatial gradient reconstruction of nonlinear aeroelastic gust response. 12th AIAA Aviation Technology, Integration, and Operations (ATIO) Conference and 14th AIAA/ISSMO Multidisciplinary Analysis and Optimization Conference, Indianapolis, Indiana, pp 5597, 2012.
- [9] Canfield R A and Sandler D A. Continuum shape sensitivity analysis for aeroelastic gust using an arbitrary lagrangian-eulerian reference frame. *Structural and Multidisciplinary Optimization*, Springer Vol. 57, pp 1871-1887, 2018.
- [10] Maute K and Lesoinne M and Farhat C. Optimization of aeroelastic systems using coupled analytical sensitivities. *38th Aerospace Sciences Meeting and Exhibit*, Reno, Nevada, pp 560, 2000.
- [11] Maute K and Nikbay M and Farhat C. Coupled analytical sensitivity analysis and optimization of three-dimensional nonlinear aeroelastic systems. *AIAA journal*, Vol. 39, No. 11, pp 2051-2061, 2001.
- [12] Maute K, Nikbay M and Farhat C. Sensitivity analysis and design optimization of three-dimensional non-linear aeroelastic systems by the adjoint method. *International Journal for Numerical Methods in Engineering*, Wiley Online Library, Vol. 56, No. 6, pp 911-933, 2003.
- [13] Blair M, Canfield R A and Roberts Jr R W. Joined-wing aeroelastic design with geometric nonlinearity. *Journal of Aircraft*, Vol. 42, No. 4, pp 832-848, 2005.
- [14] Stewart E C, Patil M J, Canfield R A and Snyder R D. Aeroelastic shape optimization of a flapping wing. *Journal of Aircraft*, AIAA, Vol. 53, No. 3, pp 636-650, 2016.
- [15] Walker W, Patil M and Canfield R. Aeroelastic tailoring of flapping membrane wings for maximum thrust and propulsive efficiency. 12th AIAA Aviation Technology, Integration, and Operations (ATIO) Conference and 14th AIAA/ISSMO Multidisciplinary Analysis and Optimization Conference, Indianapolis, Indiana, pp 5693, 2012.
- [16] Gill P E, Murray, W and Wright, M H. Practical optimization. SIAM, 2019.
- [17] Haftka R T and Gürdal Z. *Elements of structural optimization*. 1st edition, Springer Science & Business Media, 2012.

- [18] lott J, Haftka R T and Adelman H M. Selecting step sizes in sensitivity analysis by finite differences. *NASA Technical Memorandum*, 1985.
- [19] Martins J, Sturdza P and Alonso J J. The complex-step derivative approximation. *ACM Transactions on Mathematical Software (TOMS)*, Vol. 29, No. 3, pp 245-262, 2003.
- [20] Rall L B, Jones B and Corliss G F. An introduction to automatic differentiation. *Computational Differentiation: Techniques, Applications, and Tools*, Vol. 89, pp 1-18, 1996.
- [21] Margossian C C. A review of automatic differentiation and its efficient implementation. *Wiley interdisci*plinary reviews: data mining and knowledge discovery, Vol. 9, No. 4, 2019.
- [22] Liu S, and Canfield R A. Equivalence of continuum and discrete analytic sensitivity methods for nonlinear differential equations. *Structural and Multidisciplinary Optimization*, Vol. 48, pp 1173-1188, 2013.
- [23] Gagliardi G M, Kulkarni M D and Marulo, F. Continuum and Discrete Analytical Methods for Vibration and Buckling Eigenvalues Shape Sensitivities. *Aerotecnica*, Springer, 2024.
- [24] Barthelemy B and Haftka R T. Accuracy Analysis of the Semi-Analytical Method for Shape Sensitivity Calculation. *Mechanics of structures and machines*, Vol. 18, No. 3, pp 407-432, 1990.
- [25] Adhikari S and Friswell M I. Calculation of eigensolution derivatives for nonviscously damped systems. *AIAA journal*, Vol. 44, No. 8, pp 1799-1806, 2006.
- [26] Xu Z H, Zhong H X, Zhu X W and Wu B S. An efficient algebraic method for computing eigensolution sensitivity of asymmetric damped systems. *Journal of Sound and Vibration*, Elsevier, Vol. 327, pp 584-592, 2009.
- [27] Xie H. Simultaneous iterative method for the derivatives of several eigenpairs of unsymmetric damped systems. *Mechanical Systems and Signal Processing*, Elsevier, Vol. 64, pp 377-384, 2015.
- [28] Murthy D V and Haftka R T. Derivatives of eigenvalues and eigenvectors of a general complex matrix. International Journal for Numerical Methods in Engineering, Wiley Online Library, Vol. 26, No. 2, pp 293-311, 1988.
- [29] Nelson R B. Simplified calculation of eigenvector derivatives. *AIAA journal*, Vol. 14, No. 9, pp 1201-1205, 1976.
- [30] Rodden W P and Johnson E H. *MSC/NASTRAN aeroelastic analysis: user's guide.* MacNeal-Schwendler Corporation, 1994.
- [31] Adhikari, S. Derivative of eigensolutions of nonviscously damped linear systems. *AIAA journal*, Vol. 40, No. 10, pp 2061-2069, 2002.
- [32] Gagliardi G M, Kulkarni M D and Marulo, F. Continuum sensitivity analysis and improved Nelson's method for beam shape eigensensitivities. *Materials Research Proceedings, IV Aerospace PhD-Days*, Scopello (IT), Vol. 42, paper number, pp 38-42, 2024. DOI: https://doi.org/10.21741/9781644903193-9
- [33] Dailey R L. Eigenvector derivatives with repeated eigenvalues. AIAA journal, Vol. 27, No. 4, pp 486-491, 1989.
- [34] Albano E and Rodden W P. A doublet-lattice method for calculating lift distributions on oscillating surfaces in subsonic flows. *AIAA journal*, Vol. 7, No. 2, pp 279-285, 1969.